

Breaking of \mathcal{PT} Symmetry in Bounded and Unbounded Scattering Systems

Philipp Ambichl,^{1,*} Konstantinos G. Makris,^{1,2} Li Ge,³ Yidong Chong,⁴ A. Douglas Stone,⁵ and Stefan Rotter^{1,†}

¹*Institute for Theoretical Physics, Vienna University of Technology, A-1040 Vienna, Austria, EU*

²*Department of Electrical Engineering, Princeton University, Princeton, New Jersey 08544, USA*

³*Department of Engineering Science and Physics, College of Staten Island, CUNY, New York 10314, USA*

⁴*Division of Physics and Applied Physics, Nanyang Technological University, Singapore 637371, Singapore*

⁵*Department of Applied Physics, Yale University, New Haven, Connecticut 06520, USA*

(Received 16 July 2013; revised manuscript received 1 November 2013; published 18 December 2013)

\mathcal{PT} -symmetric scattering systems with balanced gain and loss can undergo a symmetry-breaking transition in which the eigenvalues of the nonunitary scattering matrix change their phase shifts from real to complex values. We relate the \mathcal{PT} -symmetry-breaking points of such an unbounded scattering system to those of the underlying bounded systems. In particular, we show how the \mathcal{PT} thresholds in the scattering matrix of the unbounded system translate into analogous transitions in the Robin boundary conditions of the corresponding bounded systems. Based on this relation, we argue and then confirm that the \mathcal{PT} transitions in the scattering matrix are, under very general conditions, entirely insensitive to a variable coupling strength between the bounded region and the unbounded asymptotic region, a result that can be tested experimentally and visualized using the concept of Smith charts.

DOI: [10.1103/PhysRevX.3.041030](https://doi.org/10.1103/PhysRevX.3.041030)

Subject Areas: Photonics, Quantum Physics

One of the postulates of quantum mechanics is that Hamiltonians are Hermitian operators, which is justified by the need for real eigenvalue spectra. Some years ago, Bender and co-workers [1,2] pointed out that a whole class of “ \mathcal{PT} -symmetric” Hamiltonians also possess real spectra, despite being non-Hermitian [3,4]. This insight has initiated a remarkable surge of research activity, much of it focusing on the ability of such Hamiltonians to undergo “spontaneous \mathcal{PT} -symmetry-breaking” transitions between real and complex (conjugate-pair) eigenvalues [2,5–9]. Although the applicability of \mathcal{PT} -symmetric Hamiltonians to quantum mechanics remains speculative, it was realized beginning in 2007 that such Hamiltonians can be studied using optical waveguides and waveguide lattices, where \mathcal{PT} -symmetric non-Hermiticity may be implemented with spatially balanced gain and loss [10–12]. Based on these ideas, the \mathcal{PT} -breaking transition has now been demonstrated in a variety of experimental systems [13–19] and was predicted to occur in several more [20–27].

The use of optical waveguides was motivated by the fact that the Schrödinger equation formally maps onto the paraxial equation of diffraction describing the propagation of transverse waveguide-mode envelopes [10,11], with the z axis playing the role of the time variable, and the \mathcal{PT} -breaking transition corresponding to that of the one- or two-dimensional bounded Schrödinger problem in the

transverse direction. Subsequently, several authors studied electromagnetic scattering for the Helmholtz equation in an unbounded domain with a \mathcal{PT} -symmetric scatterer, having balanced gain and loss around at least one symmetry plane. For these systems that, in general, do not map onto a bounded Schrödinger problem [20,28–33], it was recently pointed out [20,34] that the relevant \mathcal{PT} transition occurs in the eigenvalues of the scattering (S) matrix, which relates incoming to outgoing flux channels. Specifically, it was shown that when the S matrix undergoes \mathcal{PT} -symmetry breaking, its eigenvalues go from unimodular values, lying on the complex unit circle, to inverse-conjugate pairs of complex values. This \mathcal{PT} transition in the scattering problem thus raises the question of what relation it might have to a corresponding transition in bounded Hamiltonian systems of the type studied previously. A recent study of conservation laws in such \mathcal{PT} -scattering systems suggests that a connection to the finite system with Dirichlet boundary conditions exists [34].

In this article, we derive an explicit relationship between the \mathcal{PT} -breaking transitions of bounded and unbounded systems. Specifically, we show that the regions of the phase diagram in which an unbounded system’s S matrix has either unimodular eigenvalues (\mathcal{PT} -unbroken phase) or eigenvalues with a modulus different from 1 (\mathcal{PT} -broken phase) correspond exactly to the regions in which a whole family of associated bounded systems possess specific \mathcal{PT} -symmetric or non- \mathcal{PT} -symmetric Robin-type boundary conditions (BCs), respectively. This entry will also provide an interesting way to introduce Smith charts, familiar to microwave practitioners, into our description. The importance of Robin BCs for relating the bounded and unbounded problems was noted earlier by Smilansky and co-workers [35,36]; Robin BCs in the context of \mathcal{PT}

*philipp.ambichl@tuwien.ac.at

†stefan.rotter@tuwien.ac.at

symmetry were studied by Krejčířik and co-workers [37–40]; however, the correspondence which we demonstrate in the following has not been shown previously. Although our proof will be presented in the context of the electromagnetic Helmholtz equation, it is also applicable to the Schrödinger equation and to other linear wave equations. We also find the surprising but closely related result that the transition line at which the S matrix undergoes \mathcal{PT} breaking is unchanged by adding arbitrary \mathcal{P} -symmetric layers (“mirrors”) outside the original scatterer. In other words, the transition is determined entirely by the \mathcal{PT} -symmetric inner portion of the optical structure.

Consider, as a starting point, the one-dimensional (1D) \mathcal{PT} -symmetric scatterer shown in Fig. 1(a), which is similar to those used in previous studies [20,21]. This scattering system consists of a cavity, to which two semi-infinite leads of uniform real refractive index are attached on the left and right. The cavity itself consists of three layers, one with loss (L), one with gain (G), and an air gap in the middle. Its refractive index satisfies the \mathcal{PT} -symmetry relation $n(x) = n^*(\mathcal{P}x)$, where in this case the parity operator \mathcal{P} performs a spatial reflection about $x = L/2$. We take the refractive index to be $n = n_0 + ig$ ($n = n_0 - ig$) in the loss (gain)

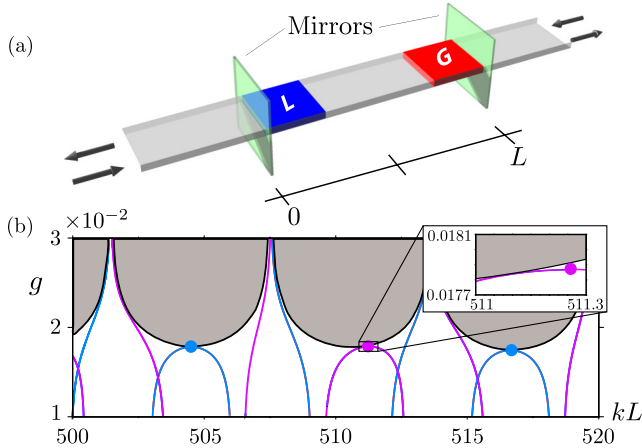


FIG. 1. (a) One-dimensional scattering system featuring a layer of loss (blue region) and gain (red region), separated by an air gap (the real part of the refractive index $n_0 = 1$ throughout). A variable coupling strength between the cavity and the asymptotic region can be introduced by two semitransparent mirrors (green regions). (b) Regions of unbroken (white) and broken (gray) \mathcal{PT} symmetry for the scattering matrix of the system displayed in (a). (\mathcal{P} denotes spatial reflection at $x = L/2$.) The “exceptional line” (black) at the boundary between these two regions contains all the \mathcal{PT} -breaking points in the scattering-matrix eigenvalues occurring at specific values of kL and strength of loss and gain g . Embedding into this plot also the (real) eigenvalues below threshold of the Helmholtz equation in the bounded domain with Dirichlet (blue lines) or Neumann (purple lines) BCs imposed at $x = 0, L$, we find that the symmetry-breaking points of these eigenvalues (see the colored dots) lie in close vicinity but not exactly on the exceptional line of the S -matrix eigenvalues (see the inset).

regions and $n = 1$ in the air gap and in the leads. The real parameter g controls the magnitude of the balanced gain and loss. The harmonic electric field E transverse to the propagation axis satisfies the Helmholtz equation

$$[\partial_x^2 + n^2(x)k^2]E(x, k) = 0, \quad (1)$$

with $k = \omega/c$; solutions to this unbounded problem exist for all $k \in \mathbb{R}$. In the leads, E can be expanded into incoming and outgoing waves:

$$E(x, k) = \begin{cases} v_1 e^{ikx} + u_1 e^{-ikx} & x \leq 0 \\ v_2 e^{-ik(x-L)} + u_2 e^{ik(x-L)} & x \geq L, \end{cases} \quad (2)$$

where L is the length of the cavity. The wave amplitudes $\{\vec{u}, \vec{v}\}$ are related by the scattering matrix $\vec{u} = S\vec{v}$. As noted, one can show [20,32] that either the eigenvalues of S are unimodular, in which case each eigenvector \vec{v}_j is \mathcal{PT} symmetric ($\mathcal{P}\vec{v}_j^* \propto \vec{v}_j$), or the eigenvalues are inverse conjugates, in which case the eigenvectors break \mathcal{PT} symmetry ($\mathcal{P}\vec{v}_1^* \propto \vec{v}_2$). The \mathcal{PT} -phase diagram (i.e., the $kL - g$ parameter space) of the scatterer is shown in Fig. 1(b). The \mathcal{PT} -symmetric part of the diagram is shown in white, and the \mathcal{PT} -broken part is shown in gray. These two regions are separated by an exceptional line (black), which marks the threshold of the \mathcal{PT} -breaking transition; everywhere on this line, the S matrix is defective [9,20]. (Its eigenvectors are linearly dependent, and it cannot be diagonalized.) Strictly speaking, due to dispersion, exact \mathcal{PT} symmetry cannot hold as k is varied over an interval [41]; hence, we imagine varying the parameters L and g to probe the \mathcal{PT} -breaking transition [42].

Our goal is to relate the physics of the unbounded scattering problem to that of a bounded system with the same complex refractive index $n(x)$, defined in the finite domain $x \in [0, L]$, and appropriate BCs at $x = 0, L$. In case this BC is itself \mathcal{PT} symmetric, the corresponding \mathcal{PT} -symmetric bounded problem will undergo a transition in which its discrete eigenvalues k_m will go from being real to being complex-conjugate pairs. The work of Ref. [34] examined the case of Dirichlet BCs and found a rough correspondence, for a given value of g , between the points at which the k_m are real and the intervals over which the \mathcal{PT} symmetry of the S matrix in the unbounded problem is unbroken. In Fig. 1(b), we plot the trajectories of the real eigenvalues k_m as a function of g for both the case of Dirichlet and of Neumann BCs; as is well known, pairs of such eigenvalues eventually meet at exceptional points of the bounded problem as the \mathcal{PT} transition occurs. (We do not plot them after they become complex.) While the exceptional points of these specific bounded problems occur near the exceptional lines of the unbounded problem, close inspection shows that they do not typically occur on the exceptional lines. We now show that a more subtle relationship exists between the bounded and unbounded problems.

Consider an incident pair of waves \vec{v} corresponding to an eigenvector of the S matrix, denoted as \vec{v}_i , with complex eigenvalue σ_i :

$$S \begin{pmatrix} v_{i,1} \\ v_{i,2} \end{pmatrix} = \begin{pmatrix} u_{i,1} \\ u_{i,2} \end{pmatrix} = \sigma_i \begin{pmatrix} v_{i,1} \\ v_{i,2} \end{pmatrix}. \quad (3)$$

Let $\psi_i(x)$ denote the corresponding field, obtained by inserting the coefficients of \vec{v}_i and \vec{u}_i into Eq. (2) and by solving Eq. (1). At the boundaries $x = 0, L$, this scattering eigenfunction must obey

$$\psi_i(0) = v_{i,1}(1 + \sigma_i), \quad -\partial_x \psi_i(0) = -v_{i,1}ik(1 - \sigma_i), \quad (4)$$

$$\psi_i(L) = v_{i,2}(1 + \sigma_i), \quad \partial_x \psi_i(L) = -v_{i,2}ik(1 - \sigma_i). \quad (5)$$

We now ask what choice of BC a bounded system must have in order to possess an eigenfrequency k_m that is equal to the value of k chosen for the unbounded system. Note that for this BC, the eigenfunction $E_m(x)$ also coincides with the scattering field $\psi_i(x)$ within the scatterer $x \in [0, L]$. It is easy to see that Eqs. (4) and (5) define Robin BCs of the form

$$-\partial_x \psi_i(0) = \lambda \psi_i(0), \quad \partial_x \psi_i(L) = \lambda \psi_i(L), \quad (6)$$

where the Robin parameter λ is related to σ_i by

$$\lambda_i(\sigma_i) = ik \frac{\sigma_i - 1}{\sigma_i + 1} \iff \sigma_i(\lambda_i) = \frac{ik + \lambda_i}{ik - \lambda_i}. \quad (7)$$

We have thus found, by construction, an exact mapping between one of the scattering eigenstates of the unbounded system, at any arbitrary wave vector k and gain-loss parameter g , and a particular eigenstate of a specific bounded system with a Robin BC whose eigenfrequency equals k at the same value of g . Since the S matrix depends parametrically on k and g , the relevant bounded system has a different BC at each point in the phase diagram and a real eigenfrequency $k_m = k$. Furthermore, the construction also works in the opposite direction: Given any bounded problem obeying the BC (6) and a choice of any one of its real eigenfrequencies k_m , the corresponding scattering matrix $S(k_m, g)$ must have an eigenvalue given by the right-hand expression in Eq. (7). This mapping is completely general for any 1D Helmholtz equation and $n(x)$; we did not use Hermiticity or \mathcal{PT} symmetry in deriving Eq. (7). A transformation very similar to Eq. (7) is, in fact, used extensively in microwave engineering and known there under the name of ‘‘Smith charts’’ [43,44]. This concept maps the normalized impedance z of a one-port system (one input, one output port) to its reflection coefficient ρ through a Möbius transformation $\rho = (z - 1)/(z + 1)$. Rewriting Eq. (7) as $-\sigma_i = (i\lambda/k - 1)/(i\lambda/k + 1)$, we immediately see the equivalence of the two transformations if we interpret $-\sigma_i$ as ρ (the minus sign is due to our convention for the S matrix) and $i\lambda/k$ as z . Note, however, that differently from the conventional concept of Smith

charts, our approach from above applies to systems with an arbitrary number of ports. What we thus find is that a subdivision of a multiport scattering problem into independent scattering-matrix eigenchannels allows us to assign to each of these channels its own single-port Möbius transformation and with it a corresponding Smith chart. We speculate that this approach might also find applications in multiport microwave scattering problems.

For the \mathcal{PT} -symmetric case considered here, the mapping (7) has the following immediate implications: In the \mathcal{PT} -symmetric phase of the S matrix, both σ_i 's are unimodular and the λ_i 's are real. In this case, the Möbius transformation in Eq. (7) maps values of σ on the complex unit circle onto the entire real λ axis and vice versa. With real λ_i , the Robin BCs are Hermitian and satisfy \mathcal{P} and \mathcal{T} symmetry separately, even though the heterostructure itself does not. It follows that the union of the trajectories of all real eigenvalues k_m in the bounded \mathcal{PT} problem coincides with the unimodular phase of S in the $kL - g$ plane, as the real λ varies from $-\infty$ to ∞ and g varies from zero to ∞ . Thus, there is no simple correspondence between the \mathcal{PT} transition in scattering and any specific bounded problem; each bounded problem, however, contains information about the \mathcal{PT} -phase diagram. This statement is illustrated in Figs. 2(a) and 2(b), in which we vary g up to the transition point of the bounded system for many different real values of λ and for two different \mathcal{PT} structures of increasing complexity.

Note that the above statement does not imply that the phase boundary of the \mathcal{PT} -scattering problem (every point of which is an exceptional point of S) coincides with the union of all exceptional points of the bounded

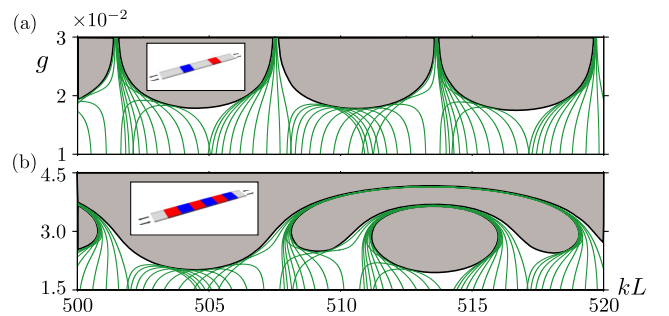


FIG. 2. Eigenvalues k_n (green lines) of the Helmholtz equation [Eq. (1)] in the bounded domain, with Robin BCs as defined in Eq. (7). Only the real eigenvalues below the \mathcal{PT} threshold are shown as a function of the gain or loss parameter g . (Altogether, ten different values of the boundary parameter $\lambda \in [-500, +500]$ are used.) The envelope of the eigenvalues in this bounded system corresponds exactly to the exceptional line (black), which separates the unbroken (white regions) from the broken (gray regions) \mathcal{PT} phases in the corresponding unbounded scattering problem. Results are shown for (a) a two-layer setup as displayed in Fig. 1(a) as well as for (b) a more complicated system featuring altogether six layers of loss and gain (see the insets).

problem [see the inset in Fig. 1(b)]. Since the latter points cannot occur in the \mathcal{PT} -broken phase of S , they are, however, enclosed by the phase boundary of S . In the \mathcal{PT} -broken phase of S , the σ_i have left the unit circle and the two corresponding λ_i form a complex-conjugate pair at each point in the $kL - g$ plane. Whereas the BCs are then non-Hermitian and non- \mathcal{PT} -symmetric, the equivalence between the bounded and the unbounded quantities $k_m = k$, $E_m(x) = \psi_i(x)$, still holds and may be visualized using the concept of 3D Smith charts recently introduced in Ref. [44]. Note how, in this way, the bounded-unbounded mapping from above provides important information on the boundary between phases where the scattering matrix features eigenvalues on or away from the unit circle, respectively. The more trivial cases are realized for Hermitian systems, where the scattering-matrix eigenvalues are always on the unit circle, or for systems with only gain or only loss, where these eigenvalues never fall on the unit circle.

The mapping between bounded and unbounded problems suggests a further, previously unknown property of the \mathcal{PT} transition in scattering. This property can be uncovered by observing that adding thin regions of a real index of refraction (like a delta function) to the scattering region symmetrically at each end (which preserves \mathcal{PT} symmetry) does not change the scattering-matrix eigenstates inside the mirrors (apart from a global amplitude). Instead, the mirrors just shift the boundary parameter λ of the corresponding bounded problem without mirrors by a real value $\lambda \rightarrow \tilde{\lambda} = \lambda + \mu$, $\mu \in \mathbb{R}$ (where μ just depends on the reflectivity of the mirror). Changing the BC in this sense, however, does not change the location of the exceptional line since the \mathcal{PT} -symmetric phase of S is the union of all real values of λ as mentioned, from $-\infty$ to ∞ . This result can be conveniently visualized with a Smith chart (see Fig. 3), where the shift of λ can be seen to just rotate both scattering-matrix eigenvalues on the unit circle, which leaves the gain or loss strength g at which they coalesce invariant [compare Figs. 3(a) and 3(b)]. We thus arrive at the conjecture that many different \mathcal{PT} -scattering problems have the same \mathcal{PT} -phase diagram, if they differ only by the addition of dielectric mirrors at the two ends. This conjecture can be proven rigorously in 1D for arbitrary lossless dielectric structures added to the original \mathcal{PT} cavities. (See Appendix A for this proof, which also holds for thick dielectric structures featuring several dielectric layers.) We have also tested this “mirror theorem” numerically by adding lossless mirrors [see Fig. 1(a)] to the ends of the six-layer scattering system in Fig. 2(b), and find that its complicated phase boundary is reproduced to within the numerical accuracy of the computation.

The above mirror theorem also features an interesting manifestation in the ratio of the incoming (outgoing) amplitudes $\xi_i \equiv v_{i,1}/v_{i,2} (= u_{i,1}/u_{i,2})$ of the scattering eigenstates in 1D, whose modulus and phase display a

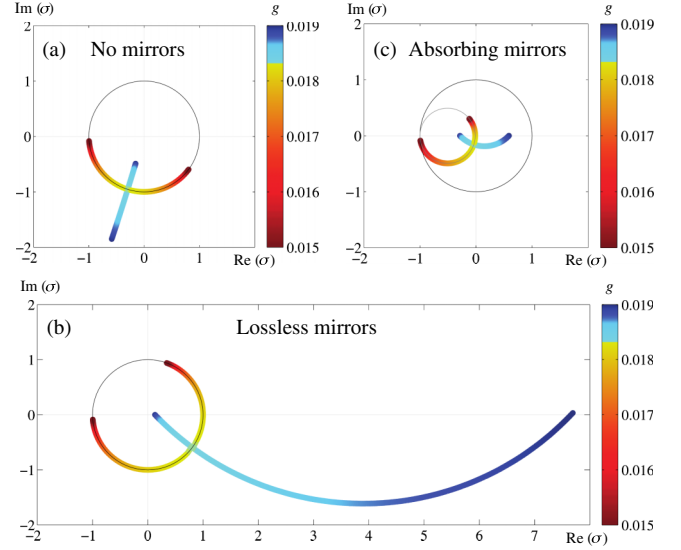


FIG. 3. Movement of the scattering-matrix eigenvalues σ_i for the \mathcal{PT} -scattering system shown in Fig. 1(a) as a function of the gain-loss strength g (see the color bars on the right-hand sides of the panels) and at $k = 515.0$. (a) The case without externally placed mirrors where two σ_i move on the unit circle and coincide at a critical value of g (see the color bar on the side). (b) Placing thin dielectric mirrors symmetrically around the gain-loss region rotates the σ_i on the unit circle (below threshold) but leaves the critical gain-loss strength at which they coalesce invariant. (c) We have added the same degree of absorption to both mirrors, which shrinks the circle on which the σ_i rotate (below threshold) to a smaller circle that touches the unit circle at $\sigma = -1$ and that has its center on the real axis. Also, in this case, the critical gain-loss strength at which the two σ_i coalesce is the same as in (a) and (b).

bifurcation at the phase boundary of S , respectively [34]. As we show in Appendix A, ξ_i is invariant not just at the exceptional line with the addition of lossless symmetric mirrors; it is so everywhere in the phase space, both in the \mathcal{PT} -symmetric phase and the broken phase. More surprisingly, this property holds even when the symmetric mirrors added are dissipative or amplifying, which clearly violates the global \mathcal{PT} symmetry of the heterostructure. This finding implies that the phase boundary of S is also invariant in this general situation, and we find, indeed, that the scattering eigenvalues σ_i still meet at exactly the same exceptional line as in the case without such mirrors. For thin non-Hermitian mirrors with loss or gain, this situation can again be understood by the shift that these mirrors induce on the Robin BC parameter $\lambda \rightarrow \tilde{\lambda} = \lambda + \mu$, with μ now being complex rather than real as before. As visualized conveniently on a Smith chart, the real part of μ leads again to a rotation of the scattering-matrix eigenvalues σ_i , but its imaginary part shrinks (expands) the circle below (beyond) the unit circle on which they rotate in the \mathcal{PT} -unbroken phase [see Fig. 3(c)]. Both of these operations do, however, leave the critical gain or loss strength g

at which the two scattering-matrix eigenvalues σ_i coalesce invariant. Since both the scattering eigenvectors and eigenvalues still coalesce at the original exceptional line, we arrive at the very general result that this line is entirely unaffected by the symmetric mirrors, even if they are absorbing or amplifying. In Appendix A, we provide a rigorous proof of this result even for thick stacks of absorbing or amplifying mirrors and also check this result explicitly numerically. The generalization of the mirror theorem to non-Hermitian mirrors is particularly important for two reasons: First, it shows that the exceptional points in a \mathcal{PT} -symmetric system are not necessarily a result of the global \mathcal{PT} symmetry; they persist even when the symmetry is broken when the absorptive or amplifying mirrors are added. Second, it paves the way for the experimental verification of the mirror theorem, since in practice, the mirrors can never be absolutely loss free.

Our mapping approach to connecting bounded and unbounded scattering problems suggests that some form of the mirror theorem could also hold in higher dimensions; we will now demonstrate a two-dimensional example. (Some general relations that hold for arbitrary 2D \mathcal{PT} -symmetric scattering problems are provided in Appendix C.) Consider the case of a two-dimensional \mathcal{PT} -symmetric disk of radius R , as shown in Fig. 4(a). To evaluate a scattering matrix for such a system, we envision a circular boundary with radius $B > R$ [see Fig. 4(a)] outside of which we define an appropriate scattering basis as the product of normalized incoming (-) and outgoing (+)

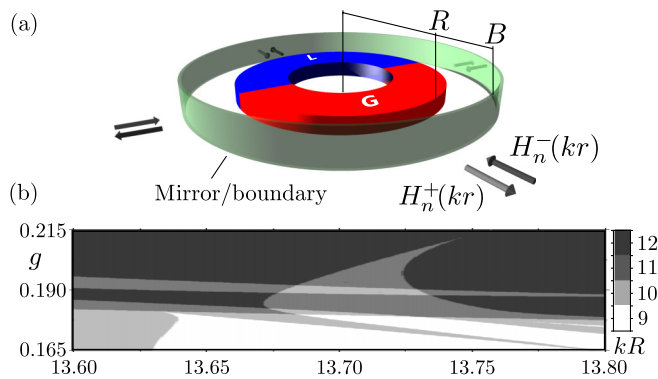


FIG. 4. (a) \mathcal{PT} -symmetric disk of radius R consisting of one region with loss (blue) and one with gain (red), enclosing an air gap ($n_0 = 1$ throughout). As in 1D, a partially transparent mirror (green region) can be used to vary the coupling strength to the asymptotic region. (b) A small part of the complicated phase diagram with overlapping phases of broken and unbroken \mathcal{PT} symmetry for the S -matrix eigenstates in this system. Different shades of gray correspond to different numbers of pairs of scattering-matrix eigenvalues in their respective \mathcal{PT} -broken phases. As we verified explicitly with our numerical simulations for this device, the phase diagram stays unchanged when tuning the reflectivity of the mirror placed in the far field. (We choose a value $B = 1000 \times R$.)

Hankel functions $H_n^\pm(kr) \equiv H_n^\pm(kr)/H_n^\pm(kB)$ and normalized trigonometric functions $\chi_{n,1}(\varphi) = A_1 \sin(n\varphi)$ and $\chi_{n,2}(\varphi) = A_2 \cos(n\varphi)$. For the infinite-dimensional scattering matrix defined in this basis, there are typically many eigenvalue pairs that go through a \mathcal{PT} transition, leading to a very complicated phase diagram [a small detail of which is shown in Fig. 4(b)]. Still, we can represent the scattering eigenstates in the bounded domain $r < B$ as the eigenstates of a boundary value problem (with the boundary at $r = B$). For this purpose, we first expand the scattering-matrix eigenstates $S\vec{v}_i = \sigma_i \vec{v}_i$ for $r > B$ in the above basis $\psi_i = \sum_{n,\eta} v_{n,\eta}^i \chi_{n,\eta} (H_n^- + \sigma_i H_n^+)$. Making a Robin ansatz for the boundary conditions of these states ψ_i (as in 1D),

$$\partial_r \psi_i(\vec{x}) = \lambda_i \psi_i(\vec{x}), \quad \lambda_i \equiv \lambda(\sigma_i, \varphi), \quad (8)$$

we find that the corresponding factors λ_i appearing here do not, in general, just depend on the eigenvalue σ_i but also on the angular position φ on the boundary. The resulting angle-dependent Robin boundary condition takes the following form:

$$\partial_r \bar{\psi}_i(r, \varphi)|_{r=B} = \sum_{n,\eta} \Lambda_n^i \chi_{n,\eta}(\varphi) \int_0^{2\pi} d\theta \chi_{n,\eta}(\theta) \psi_i(B, \theta), \quad (9)$$

with coefficients $\Lambda_n^i = (\partial_r H_n^- + \sigma_i \partial_r H_n^+)|_{r=B} (1 + \sigma_i)^{-1}$. These coefficients do, however, lose their n dependence if we choose the boundary of our finite domain in the far field, i.e., $B \gg R$. In this case, the Hankel functions can be approximated by n -independent cylindrical waves $H_n^\pm(kr) \approx e^{\pm ik(r-B)}/\sqrt{r/B}$ for $r > B$, and the expressions in Eq. (9) drastically simplify. As a result, the terms λ_i in the Robin boundary condition [Eq. (8)] are then given by the coefficients Λ_n^i that are independent of n and thus of φ . Neglecting contributions of lower order than $r^{-1/2}$, we find

$$\lambda(\sigma_i, \varphi) \equiv \lambda_i = ik \frac{\sigma_i - 1}{\sigma_i + 1} = \text{const}, \quad (10)$$

which is exactly the same expression [Eq. (7)] that we have previously obtained in 1D. In the same way as we have argued in 1D that a mirror placed symmetrically around the \mathcal{PT} system does not change the exceptional line, we can now make the same conjecture for each individual eigenvalue of a 2D scattering matrix evaluated in the far field. Hence, the complicated \mathcal{PT} -phase diagrams as in Fig. 4(b) should not change with the addition of concentric mirrors in the far field. Again, we confirm this conjecture by numerical tests involving the structure shown in Fig. 4(a).

The mirror theorem indicates that the \mathcal{PT} transition in scattering is quite a subtle phenomenon. If we think of the \mathcal{PT} -symmetric scattering region as a resonator, adding (nonabsorbing) external mirrors greatly enhances the Q value (i.e., the cavity lifetime) of such a resonator

but apparently has no effect on its phase boundary. The reasoning that having the waves stay in the resonator much longer would allow them to feel the presence of gain and loss more strongly and would thus lead to a \mathcal{PT} transition at smaller g therefore proves incorrect. Our results thus dramatically illustrate that the \mathcal{PT} -breaking transition in scattering is not a resonance phenomenon and that it does not depend on quantities like the round-trip gain or loss that are used to estimate the lasing transition. Instead, the \mathcal{PT} transition is sensitive to the coupling of the gain and loss regions with each other, with strong coupling making the transition harder to achieve and weak coupling making it (trivially) easier. Quite on the contrary, the coupling to the external world has no effect at all on the transition but strongly affects other features of the resonator that are sensitive to higher Q values. Consider, e.g., those singular points in the broken symmetry phase [20,28,31,32,45,46] at which one eigenvalue of the 1D S matrix goes to infinity, corresponding to the laser threshold, and the other one goes to zero, corresponding to coherent perfect absorption (CPA) [20]. If one adds highly reflecting dielectric mirrors to a simple low- Q \mathcal{PT} resonator as in Fig. 1(a), these singular CPA laser points are pulled down almost to the \mathcal{PT} -phase boundary which itself, however, stays unchanged. This behavior, details of which are discussed in Appendix B, nicely illustrates that \mathcal{PT} -symmetry breaking and the lasing transition are very different phenomena.

In summary, we have uncovered a close link between the phase transitions in the scattering matrix S of an unbounded \mathcal{PT} -symmetric system and the corresponding transitions in the underlying bounded systems. The most interesting result that follows from this relation is the fact that under very general conditions, the \mathcal{PT} thresholds in the scattering matrix are unchanged by external mirrors that increase the Q values of the scattering system. This prediction should be directly testable in the \mathcal{PT} -symmetric scattering experiments that have recently been realized.

We would like to thank S. Burkhardt, R. El-Ganainy, U. Günther, and M. Liertzer for helpful discussions. Financial support by the following funding sources is gratefully acknowledged: the Vienna Science and Technology Fund (WWTF) through Project No. MA09-030 (LICOTOLI), the Austrian Science Fund (FWF) through Projects No. F25-P14 (SFB IR-ON) and No. F49-P10 (SFB NextLite), the People Programme (Marie Curie Actions) of the European Union's Seventh Framework Programme (FP7/2007-2013) under REA Grant Agreement No. PIOF-GA-2011-303228 (Project NOLACOME), the Singapore National Research Foundation under Grant No. NRFF2012-02, and the U.S. National Science Foundation under Grant No. ECCS 1068642. We are also grateful for free access to the computational resources of the Vienna Scientific Cluster (VSC).

APPENDIX A: MIRROR THEOREM FOR \mathcal{PT} -PHASE TRANSITIONS IN SCATTERING THROUGH 1D HETEROSTRUCTURES

In the main text, we argue that the exceptional line of the scattering matrix and the incoming (outgoing) amplitude ratio ξ of scattering eigenstates are strictly independent of the coupling strength to the asymptotic regions if symmetric mirrors are added at both boundaries of the 1D scattering system. Here, we prove this independence explicitly, whether or not the mirrors are lossless.

The 1D scattering matrix S connecting incoming (\vec{v}) with outgoing (\vec{u}) coefficients is defined by

$$\begin{pmatrix} u_1 \\ u_2 \end{pmatrix} = S \begin{pmatrix} v_1 \\ v_2 \end{pmatrix} \equiv \begin{pmatrix} r_L & t \\ t & r_R \end{pmatrix} \begin{pmatrix} v_1 \\ v_2 \end{pmatrix}, \quad (\text{A1})$$

where $r_{L(R)}$ denote the reflection coefficients for injection from the left (right) and t the transmission amplitude. It is easy to see that its eigenvalues and the incoming (outgoing) amplitude ratios $\xi \equiv v_1/v_2 (= u_1/u_2)$ of scattering-matrix eigenstates are given by

$$\sigma_{1,2} = \frac{r_L + r_R}{2} \pm \sqrt{\frac{(r_L - r_R)^2}{4} + t^2}, \quad (\text{A2})$$

$$\xi_{1,2} = \frac{r_L - r_R}{2t} \pm \frac{1}{t} \sqrt{\frac{(r_L - r_R)^2}{4} + t^2}, \quad (\text{A3})$$

respectively. Along the exceptional line, the two eigenvalues and eigenvectors coalesce; i.e., the square roots on the right-hand sides of Eqs. (A2) and (A3) vanish. Thus, the scattering coefficients satisfy [20]

$$Y \equiv \frac{r_L}{t} - \frac{r_R}{t} = \pm 2i \quad (\text{A4})$$

at the \mathcal{PT} -phase transition points, and we note that r_L and r_R are always π out of phase with t in a \mathcal{PT} -symmetric heterostructure. Note that Y is the sum of the two off-diagonal elements in the corresponding transfer matrix M that connects the coefficients corresponding to the asymptotic regions to the right and to the left of the heterostructure. Accordingly, M is defined by

$$\begin{pmatrix} u_1 \\ v_1 \end{pmatrix} = M \begin{pmatrix} v_2 \\ u_2 \end{pmatrix} = \begin{pmatrix} t - r_L r_R / t & r_L / t \\ -r_R / t & 1 / t \end{pmatrix} \begin{pmatrix} v_2 \\ u_2 \end{pmatrix}. \quad (\text{A5})$$

We now vary the coupling of the \mathcal{PT} -symmetric heterostructure to the unbounded asymptotic regions by introducing two symmetric mirrors of arbitrary complexity and extension (one on each side). The refractive indices n_L and n_R of the left and right mirrors satisfy $n_L(x) = n_R(\mathcal{P}x)$. We refer to the transfer matrices of the left mirror, of the original heterostructure, and of the right mirror as M_L , M , and M_R , respectively. The total transfer matrix of the new structure is then $M' = M_L M M_R$.

Using the \mathcal{P} symmetry of n_L and n_R , we find that the transfer matrices of the mirrors are connected by $M_L = PM_R^{-1}P$, where P is the matrix representation of the parity operator \mathcal{P} , given by

$$P = \begin{pmatrix} 0 & 1 \\ 1 & 0 \end{pmatrix}. \quad (\text{A6})$$

This relation leads to

$$M_L = \begin{pmatrix} m_{11} & -m_{21} \\ -m_{12} & m_{22} \end{pmatrix}, \quad (\text{A7})$$

if we write

$$M_R = \begin{pmatrix} m_{11} & m_{12} \\ m_{21} & m_{22} \end{pmatrix}. \quad (\text{A8})$$

Further, writing

$$M = \begin{pmatrix} M_{11} & M_{12} \\ M_{21} & M_{22} \end{pmatrix}, \quad M' = \begin{pmatrix} M'_{11} & M'_{12} \\ M'_{21} & M'_{22} \end{pmatrix}, \quad (\text{A9})$$

we derive

$$M'_{12} = m_{11}m_{12}M_{11} + m_{11}m_{22}M_{12} - m_{12}m_{21}M_{21} - m_{21}m_{22}M_{22}, \quad (\text{A10})$$

$$M'_{21} = -m_{11}m_{12}M_{11} - m_{12}m_{21}M_{12} + m_{11}m_{22}M_{21} + m_{21}m_{22}M_{22}. \quad (\text{A11})$$

Using the general property $\text{Det}(M_R) = m_{11}m_{22} - m_{12}m_{21} = 1$, we find

$$\begin{aligned} Y' &= M'_{12} + M'_{21} \\ &= (m_{11}m_{22} - m_{12}m_{21})(M_{12} + M_{21}) \\ &= M_{12} + M_{21} \\ &= Y. \end{aligned} \quad (\text{A12})$$

One particular implication of this relation is that the two scattering eigenvalues $\sigma_{1,2}$ still coalesce at the original exceptional line, where $Y' = Y = \pm 2i$. In addition, we note that the incoming or outgoing amplitude ratios ξ can be rewritten as $Y/2 \pm \sqrt{Y^2/4 + 1}$. Thus, they are also invariant in this case everywhere in the $kL - g$ plane and coalesce at the original exceptional line. Therefore, we come to the conclusion that the exceptional line is invariant with the addition of the symmetric mirrors.

Note that we do not impose any condition on the realness of the refractive indices n_L and n_R ; thus, the above conclusion holds for lossless mirrors, as well as for absorptive or amplifying mirrors. In the former case, where n_L and n_R are real, the system is still \mathcal{PT} symmetric and the exceptional line is still the phase boundary of the \mathcal{PT} -symmetric and broken phases of S . In the latter case, where the mirrors destroy the overall \mathcal{PT} symmetry of the resulting system, i.e., $PS^\dagger PS \neq 1$, the eigenvalues of the S matrix generally do not lie on the unit circle and no symmetry breaking occurs. Nevertheless, the same

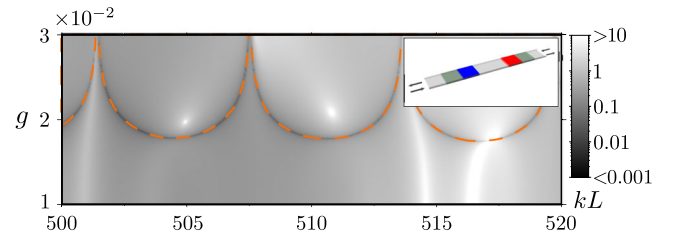


FIG. 5. Difference between the two scattering-matrix eigenvalues $D(kL, g) \equiv |\sigma_1 - \sigma_2|$ for the \mathcal{PT} -symmetric two-layer system shown in Fig. 1(a) with two slabs of width $L/4$ attached on either side (see also the smaller inset). The slabs feature randomly chosen complex refractive indices that satisfy $n_R(x) = n_L(\mathcal{P}x)$, where $R(L)$ stands for the slab on the right (left) side of the \mathcal{PT} -symmetric structure. The lines where $D = 0$, i.e., where $\sigma_1 = \sigma_2$, coincide exactly with the exceptional line of the inner \mathcal{PT} -symmetric part of the system (dashed orange line).

exceptional line persists and so do the incoming or outgoing amplitude ratios ξ everywhere in the $kL - g$ plane. To explicitly illustrate the generality of this result, we show in Fig. 5 the difference between the two scattering-matrix eigenvalues $D(kL, g) \equiv |\sigma_1 - \sigma_2|$ for a system composed of two mirrors of width $L/4$ featuring randomly chosen complex refractive-index distributions $n_L(x)$ and $n_R(x) = n_L(\mathcal{P}x)$ attached to the two-layer system displayed in Fig. 1(a). As can be seen by comparison to Fig. 1(b), the union of all the points where $D = 0$ is the exceptional line of the original system without mirrors.

APPENDIX B: DEPENDENCE OF LASING TRANSITIONS ON THE COUPLING STRENGTH FOR 1D HETEROSTRUCTURES

At discrete points in its phase space, a \mathcal{PT} -symmetric scatterer can act simultaneously as a laser at threshold and a coherent perfect absorber of incident light [20,31]. Since these CPA laser points correspond to one eigenvalue of the S matrix going to zero and the other going to infinity, they can occur only within the \mathcal{PT} -broken phase of S . Although the mirror theorem (see the main text and Appendix A) shows that adding \mathcal{P} -symmetric mirrors at the scattering boundaries does not alter the exceptional line, they do affect the position of the CPA laser points.

To demonstrate this invariance, we consider again a 1D \mathcal{PT} -symmetric scatterer (see the inset of Fig. 6) and modify its dielectric function by

$$\Delta[n^2(x)] = \mu[\delta(x) + \delta(x - L)], \quad (\text{B1})$$

with a real parameter μ that controls the mirror reflectivity. This change in the dielectric function corresponds to placing dielectric mirrors of vanishing width at the scattering boundaries $x = 0, L$. (The reason for using zero-width mirrors is to avoid the complication of additional internal resonances.)

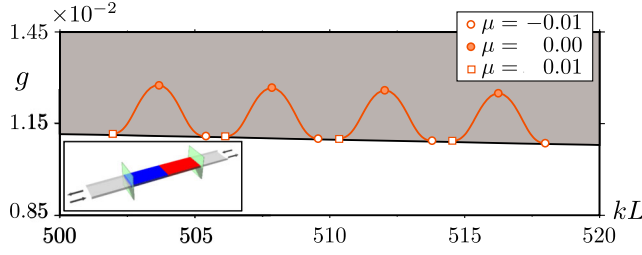


FIG. 6. CPA laser points for a \mathcal{PT} -symmetric scatterer consisting of two adjacent regions of refractive index $n = 1.5 \pm ig$, with zero-width mirrors at the scattering boundary (see the bottom left inset). The mirror parameter μ is defined in Eq. (B1). The orange curves show the trajectories of four distinct CPA laser points for varying values of μ , with the symbols indicating the positions at particular values of μ (see the top right inset). The solid black curve is the exceptional line.

Figure 6 shows the trajectories of the CPA laser points as μ is varied, for a simple heterostructure of two equal-length gain-loss segments with refractive index $n_0 \pm ig$ (and with $n = 1$ outside). For $\mu = 0$, the CPA laser points are located at some distance above the exceptional line, as discussed in Ref. [20]. Increasing or decreasing μ pulls the CPA laser points toward the exceptional line, which can be interpreted as an effect of the increase in the Q factor of the cavity.

APPENDIX C: BOUNDARY CONDITIONS FOR TWO-DIMENSIONAL SCATTERING SETUPS

In this section, we provide further details on the connection between the \mathcal{PT} thresholds in bounded and unbounded two-dimensional (2D) systems. Following the arguments for 1D setups, we will find that in 2D, appropriate Robin BCs can also be found, which give rise to eigenstates of the S matrix.

We consider an arbitrarily shaped 2D \mathcal{PT} -symmetric cavity through the boundary of which waves can go in and out from and to infinity. The m th eigenstate of the corresponding scattering matrix, written as a coefficient vector \vec{v}_m and associated with the eigenvalue σ_m , is decomposed outside the cavity into a scattering basis ϕ_n as follows:

$$\psi_m(\vec{x}) = \sum_{n=1}^N v_{m,n} [\phi_n(\vec{x}) + \sigma_m \phi_n^*(\vec{x})]. \quad (\text{C1})$$

As was shown in Ref. [20], the eigenvectors of S satisfy $\mathcal{PT}\vec{v} \propto \vec{v}$ below threshold and $\mathcal{PT}\vec{v}_m \propto \vec{v}_{m'}$ above threshold for an associated pair of eigenvectors $(\vec{v}_m, \vec{v}_{m'})$, respectively. The connection between the normal derivative and the wave function of a scattering-matrix eigenstate at the system boundary can formally be written as follows: $\psi'_m(\vec{x}) = \lambda(\sigma_m, \vec{x})\psi_m(\vec{x})$, with the functions

$$\lambda(\sigma_m, \vec{x}) = \frac{\sum_n v_{m,n} [\phi'_n(\vec{x}) + \sigma_m \phi_n^*(\vec{x})]}{\sum_l v_{m,l} [\phi_l(\vec{x}) + \sigma_m \phi_l^*(\vec{x})]}. \quad (\text{C2})$$

Below the \mathcal{PT} threshold, where $\sigma^* = \sigma^{-1}$, we can rewrite the boundary-value function $\lambda(\sigma)$ in vector notation and suppressing (\vec{x}) as follows:

$$\lambda(\sigma) = \frac{\vec{v}^T(\vec{\phi}' + \sigma\vec{\phi}^*)}{\vec{v}^T(\vec{\phi} + \sigma\vec{\phi}^*)} = \frac{\vec{v}^\dagger P(\vec{\phi}'^* + \sigma^*\vec{\phi}')}{\vec{v}^\dagger P(\vec{\phi}^* + \sigma^*\vec{\phi})} = \mathcal{P}\lambda^*(\sigma), \quad (\text{C3})$$

where we further use $P^* = P = P^T$ for the matrix representation P of the parity operator \mathcal{P} and $\vec{v}^T \propto \vec{v}^\dagger P$. Note that the action of P and taking the normal derivative commute due to the \mathcal{P} symmetry of the boundary. From Eq. (C3), we see that $\lambda(\sigma)$ is a \mathcal{PT} -symmetric function $\lambda(\sigma, \vec{x}) = \lambda^*(\sigma, \mathcal{P}\vec{x})$, leading to \mathcal{PT} -symmetric Robin boundary conditions for the wave function. Above the \mathcal{PT} threshold of an associated pair $(\sigma_m, \sigma_{m'})$ of S -matrix eigenvalues, we find for the expression of $\lambda(\sigma_{m'})$ using $\vec{v}_{m'}^T \propto \vec{v}_m^\dagger P$ and $\sigma_{m'} = 1/\sigma_m^*$

$$\begin{aligned} \lambda(\sigma_{m'}) &= \frac{\vec{v}_{m'}^T(\vec{\phi}' + \frac{1}{\sigma_m^*}\vec{\phi}^*)}{\vec{v}_{m'}^T(\vec{\phi} + \frac{1}{\sigma_m^*}\vec{\phi}^*)} = \frac{\vec{v}_m^\dagger P(\vec{\phi}'^* + \sigma_m^*\vec{\phi}')}{\vec{v}_m^\dagger P(\vec{\phi}^* + \sigma_m^*\vec{\phi})} \\ &= \mathcal{P}\lambda^*(\sigma_m). \end{aligned} \quad (\text{C4})$$

From Eqs. (C4) and (C3), we may thus conclude that for 2D \mathcal{PT} systems, the situation is very similar to the 1D case: Below the \mathcal{PT} threshold of a pair of S eigenvalues, the corresponding eigenstates feature different, \mathcal{PT} -symmetric BCs, and above threshold, the BCs are non- \mathcal{PT} -symmetric but pairwise connected.

-
- [1] C.M. Bender and S. Boettcher, *Real Spectra in Non-Hermitian Hamiltonians Having PT Symmetry*, *Phys. Rev. Lett.* **80**, 5243 (1998).
 - [2] C.M. Bender, D.C. Brody, and H.F. Jones, *Complex Extension of Quantum Mechanics*, *Phys. Rev. Lett.* **89**, 270401 (2002).
 - [3] A. Mostafazadeh, *Pseudo-Hermiticity versus PT Symmetry: The Necessary Condition for the Reality of the Spectrum of a Non-Hermitian Hamiltonian*, *J. Math. Phys. (N.Y.)* **43**, 205 (2002).
 - [4] G. Lévai and M. Znojil, *Systematic Search for \mathcal{PT} -Symmetric Potentials with Real Energy Spectra*, *J. Phys. A* **33**, 7165 (2000).
 - [5] C.M. Bender, D.C. Brody, H.F. Jones, and B.K. Meister, *Faster than Hermitian Quantum Mechanics*, *Phys. Rev. Lett.* **98**, 040403 (2007).
 - [6] C.M. Bender, G.V. Dunne, and P.N. Meisinger, *Complex Periodic Potentials with Real Band Spectra*, *Phys. Lett. A* **252**, 272 (1999).
 - [7] H.F. Jones, *The Energy Spectrum of Complex Periodic Potentials of the Kronig-Penney Type*, *Phys. Lett. A* **262**, 242 (1999).
 - [8] S. Klaiman, U. Günther, and N. Moiseyev, *Visualization of Branch Points in \mathcal{PT} -Symmetric Waveguides*, *Phys. Rev. Lett.* **101**, 080402 (2008).

- [9] W. D. Heiss, *The Physics of Exceptional Points*, *J. Phys. A* **45**, 444016 (2012).
- [10] R. El-Ganainy, K. G. Makris, D. N. Christodoulides, and Z. H. Musslimani, *Theory of Coupled Optical \mathcal{PT} -Symmetric Structures*, *Opt. Lett.* **32**, 2632 (2007).
- [11] K. G. Makris, R. El-Ganainy, D. N. Christodoulides, and Z. H. Musslimani, *Beam Dynamics in \mathcal{PT} Symmetric Optical Lattices*, *Phys. Rev. Lett.* **100**, 103904 (2008).
- [12] K. G. Makris, R. El-Ganainy, D. N. Christodoulides, and Z. H. Musslimani, *\mathcal{PT} -Symmetric Optical Lattices*, *Phys. Rev. A* **81**, 063807 (2010).
- [13] C. E. Rüter, K. G. Makris, R. El-Ganainy, D. N. Christodoulides, M. Segev, and D. Kip, *Observation of Parity-Time Symmetry in Optics*, *Nat. Phys.* **6**, 192 (2010).
- [14] A. Guo, G. J. Salamo, D. Duchesne, R. Morandotti, M. Volatier-Ravat, V. Aimez, G. A. Siviloglou, and D. N. Christodoulides, *Observation of \mathcal{PT} -Symmetry Breaking in Complex Optical Potentials*, *Phys. Rev. Lett.* **103**, 093902 (2009).
- [15] S. Bittner, B. Dietz, U. Günther, H. L. Harney, M. Miski-Oglu, A. Richter, and F. Schäfer, *\mathcal{PT} Symmetry and Spontaneous Symmetry Breaking in a Microwave Billiard*, *Phys. Rev. Lett.* **108**, 024101 (2012).
- [16] J. Schindler, A. Li, M. C. Zheng, F. M. Ellis, and T. Kottos, *Experimental Study of Active LRC Circuits with \mathcal{PT} Symmetries*, *Phys. Rev. A* **84**, 040101(R) (2011).
- [17] A. Regensburger, C. Bersch, M.-A. Miri, G. Onishchukov, D. N. Christodoulides, and U. Peschel, *Parity-Time Synthetic Photonic Lattices*, *Nature (London)* **488**, 167 (2012).
- [18] B. Peng, S. K. Ozdemir, F. Lei, F. Monifi, M. Gianfreda, G. L. Long, S. Fan, F. Nori, C. M. Bender, and L. Yang, *Nonreciprocal Light Transmission in Parity-Time-Symmetric Whispering-Gallery Microcavities*, [arXiv:1308.4564](https://arxiv.org/abs/1308.4564).
- [19] C. M. Bender, B. K. Berntson, D. Parker, and E. Samuel, *Observation of \mathcal{PT} Phase Transition in a Simple Mechanical System*, *Am. J. Phys.* **81**, 173 (2013).
- [20] Y. D. Chong, L. Ge, and A. D. Stone, *\mathcal{PT} -Symmetry Breaking and Laser-Absorber Modes in Optical Scattering Systems*, *Phys. Rev. Lett.* **106**, 093902 (2011).
- [21] M. Liertzer, L. Ge, A. Cerjan, A. D. Stone, H. E. Türeci, and S. Rotter, *Pump-Induced Exceptional Points in Lasers*, *Phys. Rev. Lett.* **108**, 173901 (2012).
- [22] T. Prosen, *\mathcal{PT} -Symmetric Quantum Liouvillean Dynamics*, *Phys. Rev. Lett.* **109**, 090404 (2012).
- [23] H. Ramezani, D. N. Christodoulides, V. Kovanis, I. Vitebskiy, and T. Kottos, *\mathcal{PT} -Symmetric Talbot Effects*, *Phys. Rev. Lett.* **109**, 033902 (2012).
- [24] E.-M. Graefe, *Stationary States of a \mathcal{PT} Symmetric Two-Mode Bose-Einstein Condensate*, *J. Phys. A* **45**, 444015 (2012).
- [25] N. Lazarides and G. P. Tsironis, *Gain-Driven Discrete Breathers in \mathcal{PT} -Symmetric Nonlinear Metamaterials*, *Phys. Rev. Lett.* **110**, 053901 (2013).
- [26] M. Kreibich, J. Main, H. Cartarius, and G. Wunner, *Hermitian Four-Well Potential as a Realization of a \mathcal{PT} -Symmetric System*, *Phys. Rev. A* **87**, 051601(R) (2013).
- [27] M. Kang, F. Liu, and J. Li, *Effective Spontaneous \mathcal{PT} -Symmetry Breaking in Hybridized Metamaterials*, *Phys. Rev. A* **87**, 053824 (2013).
- [28] A. Mostafazadeh, *Spectral Singularities of Complex Scattering Potentials and Infinite Reflection and Transmission Coefficients at Real Energies*, *Phys. Rev. Lett.* **102**, 220402 (2009).
- [29] A. Mostafazadeh, *Optical Spectral Singularities as Threshold Resonances*, *Phys. Rev. A* **83**, 045801 (2011).
- [30] F. Cannata, J.-P. Dedonder, and A. Ventura, *Scattering in \mathcal{PT} -Symmetric Quantum Mechanics*, *Ann. Phys. (Amsterdam)* **322**, 397 (2007).
- [31] S. Longhi, *\mathcal{PT} -Symmetric Laser Absorber*, *Phys. Rev. A* **82**, 031801(R) (2010).
- [32] H. Schomerus, *Quantum Noise and Self-Sustained Radiation of \mathcal{PT} -Symmetric Systems*, *Phys. Rev. Lett.* **104**, 233601 (2010).
- [33] Z. Lin, H. Ramezani, T. Eichelkraut, T. Kottos, H. Cao, and D. N. Christodoulides, *Unidirectional Invisibility Induced by \mathcal{PT} -Symmetric Periodic Structures*, *Phys. Rev. Lett.* **106**, 213901 (2011).
- [34] L. Ge, Y. D. Chong, and A. D. Stone, *Conservation Relations and Anisotropic Transmission Resonances in One-Dimensional \mathcal{PT} -Symmetric Photonic Heterostructures*, *Phys. Rev. A* **85**, 023802 (2012).
- [35] E. Doron and U. Smilansky, *Semiclassical Quantization of Chaotic Billiards: A Scattering Theory Approach*, *Nonlinearity* **5**, 1055 (1992).
- [36] M. Sieber, H. Primack, U. Smilansky, I. Ussishkin, and H. Schanz, *Semiclassical Quantization of Billiards with Mixed Boundary Conditions*, *J. Phys. A* **28**, 5041 (1995).
- [37] D. Krejčířík, H. Bíla, and M. Znojil, *Closed Formula for the Metric in the Hilbert Space of a \mathcal{PT} -Symmetric Model*, *J. Phys. A* **39**, 10143 (2006).
- [38] D. Krejčířík, *Calculation of the Metric in the Hilbert Space of a \mathcal{PT} -Symmetric Model via the Spectral Theorem*, *J. Phys. A* **41**, 244012 (2008).
- [39] D. Krejčířík and P. Siegl, *\mathcal{PT} -Symmetric Models in Curved Manifolds*, *J. Phys. A* **43**, 485204 (2010).
- [40] H. Hernandez-Coronado, D. Krejčířík, and P. Siegl, *Perfect Transmission Scattering as a \mathcal{PT} -Symmetric Spectral Problem*, *Phys. Lett. A* **375**, 2149 (2011).
- [41] A. A. Zyablovsky, A. P. Vinogradov, A. V. Dorofeenko, A. A. Pukhov, and A. A. Lisyansky, *Comment on “ \mathcal{PT} -Symmetry Breaking and Laser-Absorber Modes in Optical Scattering Systems,”* [arXiv:1205.2820](https://arxiv.org/abs/1205.2820).
- [42] K. G. Makris, P. Ambichl, L. Ge, S. Rotter, and D. N. Christodoulides (unpublished).
- [43] P. H. Smith, *Transmission-Line Calculator*, *Electronics* **12**, 29 (1939).
- [44] A. A. Müller, P. Soto, D. Dascalu, D. Neculoiu, and V. E. Boria, *A 3-D Smith Chart Based on the Riemann Sphere for Active and Passive Microwave Circuits*, *IEEE Microwave Wireless Compon. Lett.* **21**, 286 (2011).
- [45] G. Yoo, H.-S. Sim, and H. Schomerus, *Quantum Noise and Mode Nonorthogonality in Non-Hermitian \mathcal{PT} -Symmetric Optical Resonators*, *Phys. Rev. A* **84**, 063833 (2011).
- [46] J. Schindler, Z. Lin, J. M. Lee, H. Ramezani, F. M. Ellis, and T. Kottos, *\mathcal{PT} -Symmetric Electronics*, *J. Phys. A* **45**, 444029 (2012).